

*Supporting Information.*

# **Fully Transparent and Distortion-Free Monotonically Stretchable Substrate by Nanostructure Alignment**

*Jung Hur<sup>1,2</sup>, Hwaeun Park<sup>3,4</sup>, Hyeongsu Oh<sup>1,2</sup>, Sujin Jeong<sup>3,4</sup>, Jinhan Cho<sup>1,2,5</sup>, Jonghwi Lee<sup>6</sup>, Seungjun Chung<sup>7</sup>, Yongtaek Hong<sup>3,4\*</sup>, Jeong Gon Son<sup>1,2\*</sup>*

<sup>1</sup>Soft Hybrid Materials Research Center, Korea Institute of Science and Technology (KIST), Seongbuk-gu, Seoul 02792, Republic of Korea

<sup>2</sup>KU-KIST Graduate School of Converging Science and Technology, Korea University, Seongbuk-gu, Seoul 02841, Republic of Korea

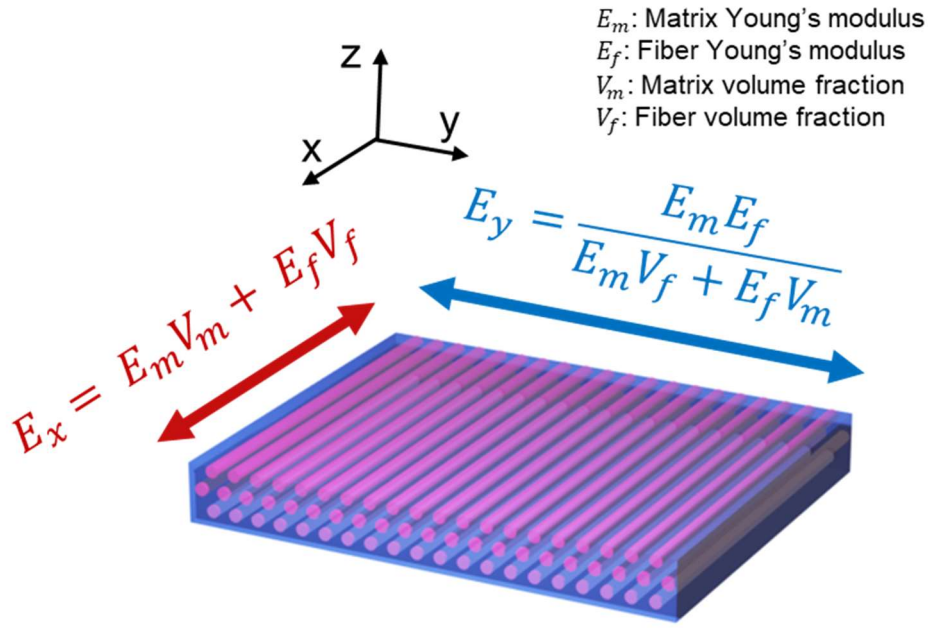
<sup>3</sup>Department of Electrical and Computer Engineering, Seoul National University, Seoul 08826, Republic of Korea

<sup>4</sup>Inter University Semiconductor Research Center (ISRC), Seoul National University, Seoul 08826, Republic of Korea

<sup>5</sup>Department of Chemical & Biological Engineering, Korea University, Seoul 02841, Republic of Korea

<sup>6</sup>School of Chemical Engineering and Materials Science, Chung-Ang University, Seoul 06974, Republic of Korea

<sup>7</sup>School of Electrical Engineering, Korea University, Seongbuk-gu, Seoul, 02841, Republic of Korea



**Figure S1.** Anisotropic modulus in aligned fiber composites

### Modulus and Poisson's ratio correlation in Transversely isotropic materials

$$\begin{bmatrix} \epsilon_{xx} \\ \epsilon_{yy} \\ \epsilon_{zz} \\ 2\epsilon_{yz} \\ 2\epsilon_{zx} \\ 2\epsilon_{xy} \end{bmatrix} = \begin{bmatrix} \frac{1}{E_x} & -\frac{\nu_{yz}}{E_y} & -\frac{\nu_{zx}}{E_z} \\ -\frac{\nu_{xy}}{E_x} & \frac{1}{E_y} & -\frac{\nu_{zy}}{E_z} \\ -\frac{\nu_{xz}}{E_x} & -\frac{\nu_{yz}}{E_y} & \frac{1}{E_z} \\ & & & \frac{1}{G_{yz}} \\ & & & & \frac{1}{G_{zx}} \\ & & & & & \frac{1}{G_{xy}} \end{bmatrix} \begin{bmatrix} \sigma_{xx} \\ \sigma_{yy} \\ \sigma_{zz} \\ \sigma_{yz} \\ \sigma_{zx} \\ \sigma_{xy} \end{bmatrix}$$

In this formulation, for any arbitrary axis  $i$  or  $j$ ,  $\epsilon_{ii}$  denotes the strain along the  $i$ -direction,  $\epsilon_{ij}$  denotes shear strain in the  $ij$ -plane,  $E_i$  is the modulus along the  $i$ -axis,  $\nu_{ij}$  is the Poisson's ratio accounting for contraction in the  $j$ -direction when tension is applied in the  $i$ -direction,  $G_{ij}$  is the shear modulus in the  $ij$ -plane,  $\sigma_{ii}$  represents the stress along the  $i$  direction, and  $\sigma_{ij}$  is the shear stress acting along the  $j$ -direction due to a force in the  $i$ -direction. The matrix on the left represents the strain vector, the middle matrix is the compliance matrix, and the matrix on the right

is the stress vector. The elements in the n-th row and m-th column of the compliance matrix are typically denoted as  $S_{nm}$ , which simplifies representation as follows :

$$\begin{bmatrix} \frac{1}{E_x} & -\frac{\nu_{yx}}{E_y} & -\frac{\nu_{zx}}{E_z} \\ -\frac{\nu_{xy}}{E_x} & \frac{1}{E_y} & -\frac{\nu_{zy}}{E_z} \\ -\frac{\nu_{xz}}{E_x} & -\frac{\nu_{yz}}{E_y} & \frac{1}{E_z} \\ & & & \frac{1}{G_{yz}} \\ & & & & \frac{1}{G_{zx}} \\ & & & & & \frac{1}{G_{xy}} \end{bmatrix} = \begin{bmatrix} S_{11} & S_{12} & S_{13} & & & \\ S_{21} & S_{22} & S_{23} & & & \\ S_{31} & S_{32} & S_{33} & & & \\ & & & S_{44} & & \\ & & & & S_{55} & \\ & & & & & S_{66} \end{bmatrix}$$

We now demonstrate that Poisson's ratio is inversely proportional to the modulus using the strain energy density  $U$ , which represents the energy density stored within the material to maintain deformation. The strain energy density is the sum of the product of the stress vector and the compliance matrix elements, divided by two:

$$U = \frac{1}{2} \int \sigma \epsilon = \frac{1}{2} (\sigma_{xx} \epsilon_{xx} + \sigma_{yy} \epsilon_{yy} + \sigma_{zz} \epsilon_{zz} + 2\sigma_{xy} \epsilon_{xy} + 2\sigma_{yz} \epsilon_{yz} + 2\sigma_{xz} \epsilon_{xz})$$

Breaking it down further:

$$U = \frac{1}{2} [\sigma_{xx}(S_{11}\sigma_{xx} + S_{12}\sigma_{yy} + S_{13}\sigma_{zz}) + \sigma_{yy}(S_{21}\sigma_{xx} + S_{22}\sigma_{yy} + S_{33}\sigma_{zz}) + \sigma_{zz}(S_{31}\sigma_{xx} + S_{32}\sigma_{yy} + S_{33}\sigma_{zz}) + S_{66}\sigma_{xy}^2 + S_{44}\sigma_{yz}^2 + S_{55}\sigma_{xz}^2]$$

By taking the partial derivative of  $U$  with respect to  $\sigma_{xx}$ , we obtain  $\epsilon_{xx}$ , the strain in the  $x$ -direction :

$$\frac{\partial U}{\partial \sigma_{xx}} = \frac{1}{2} [2\sigma_{xx}S_{11} + S_{12}\sigma_{yy} + S_{13}\sigma_{zz} + S_{21}\sigma_{yy} + S_{31}\sigma_{zz}] = \epsilon_{xx}$$

We can calculate  $\epsilon_{xx}$  using the compliance matrix as follows :

$$\epsilon_{xx} = S_{11}\sigma_{xx} + S_{12}\sigma_{yy} + S_{13}\sigma_{zz} \quad \text{and thus,}$$

$$\frac{1}{2} [2\sigma_{xx}S_{11} + S_{12}\sigma_{yy} + S_{13}\sigma_{zz} + S_{21}\sigma_{yy} + S_{31}\sigma_{zz}] = \sigma_{xx}S_{11} + \frac{1}{2}\sigma_{yy}(S_{12} + S_{21}) + \frac{1}{2}\sigma_{zz}(S_{13} + S_{31})$$

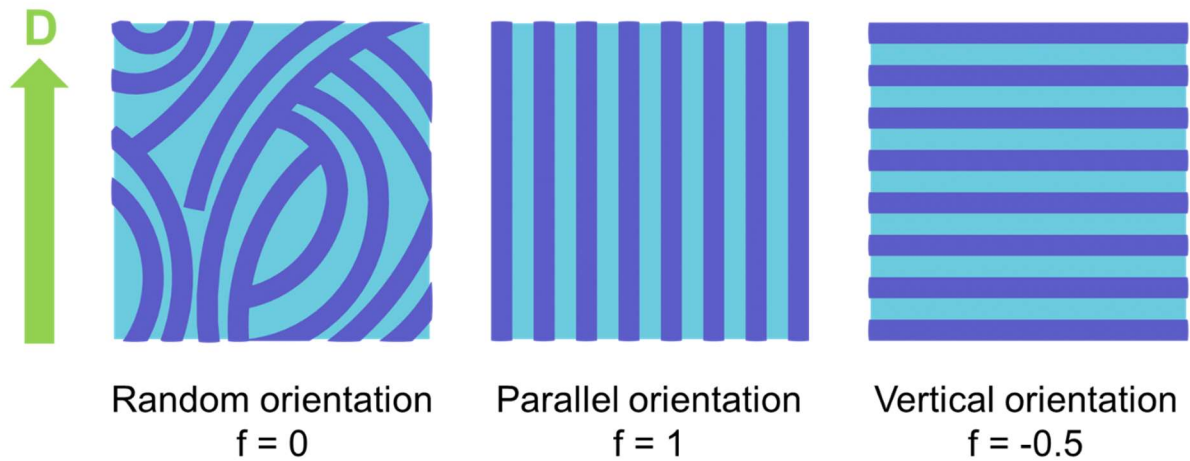
Following the conditions of identity for the coefficients of  $\sigma_{yy}$  and  $\sigma_{zz}$ :

$$S_{12} = S_{21} \text{ and } S_{13} = S_{31}$$

Substituting these elements,

$$-\frac{\nu_{yx}}{E_y} = -\frac{\nu_{xy}}{E_x}$$

For transversely isotropic materials, Poisson's ratio in the anisotropic plane is indeed inversely proportional to the modulus.



**Figure S2.** Values for the Herman's orientation parameter for random orientation, parallel orientation and vertical orientation.

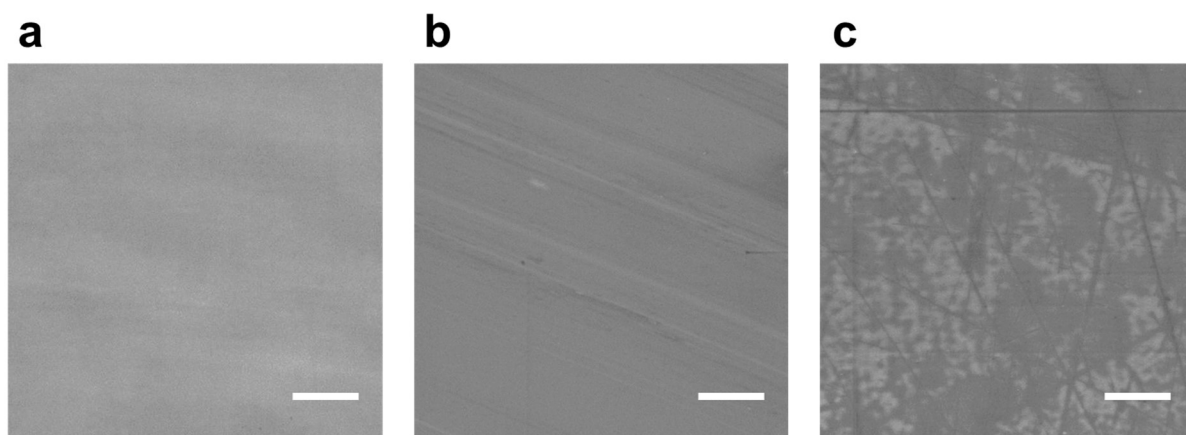
The Herman orientation factor can be calculated using the following equations:

$$f_{2D} = 2 \langle \cos^2 \theta \rangle_{2D} - 1$$

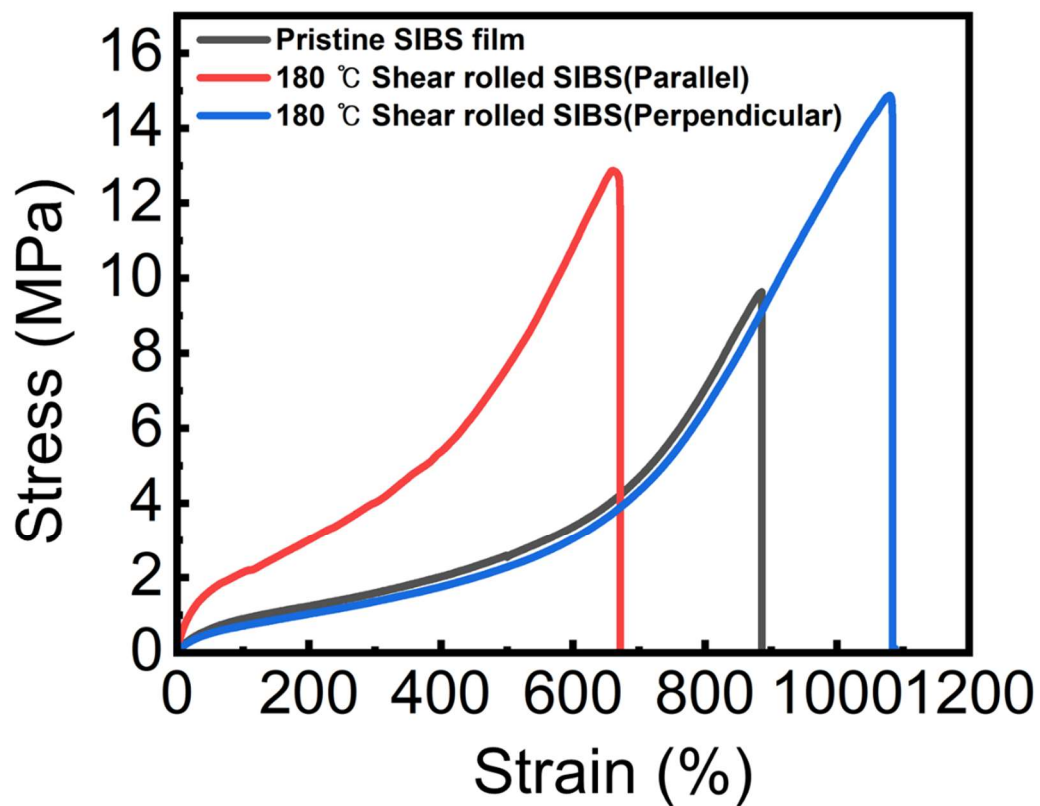
and

$$\langle \cos^2 \theta \rangle_{2D} = \frac{\int_0^\pi I(\theta)_{2D} \cos^2 \theta d\theta}{\int_0^\pi I(\theta)_{2D} d\theta},$$


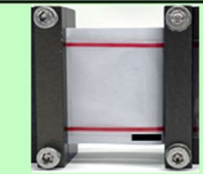
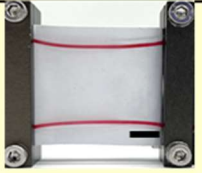
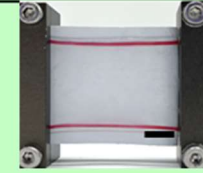
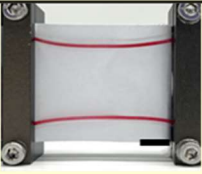
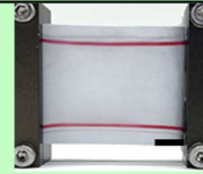
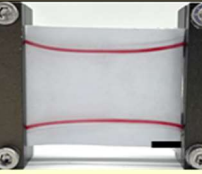
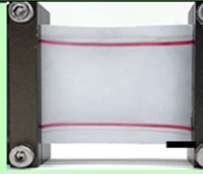

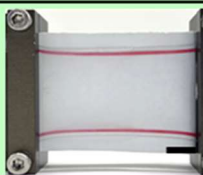
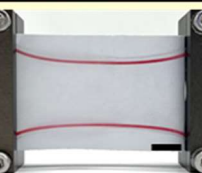

where  $\theta$  is the local orientation angle and  $I(\theta)$  is the popularity at  $\theta$ . In the figure below, the Herman orientation parameter takes a value of 0 when the domains exhibit random orientation, 1 when all domains align parallel to the direction of the arrow, and -0.5 when they are oriented vertically.



**Figure S3.** Macroscopic delamination of the shear-rolled thin SIBS films. (a) 180 °C, (b) 200 °C, and (c) 220 °C shear-rolled thin SIBS films. The white scale bar in the bottom right of the image represents 10  $\mu\text{m}$ .

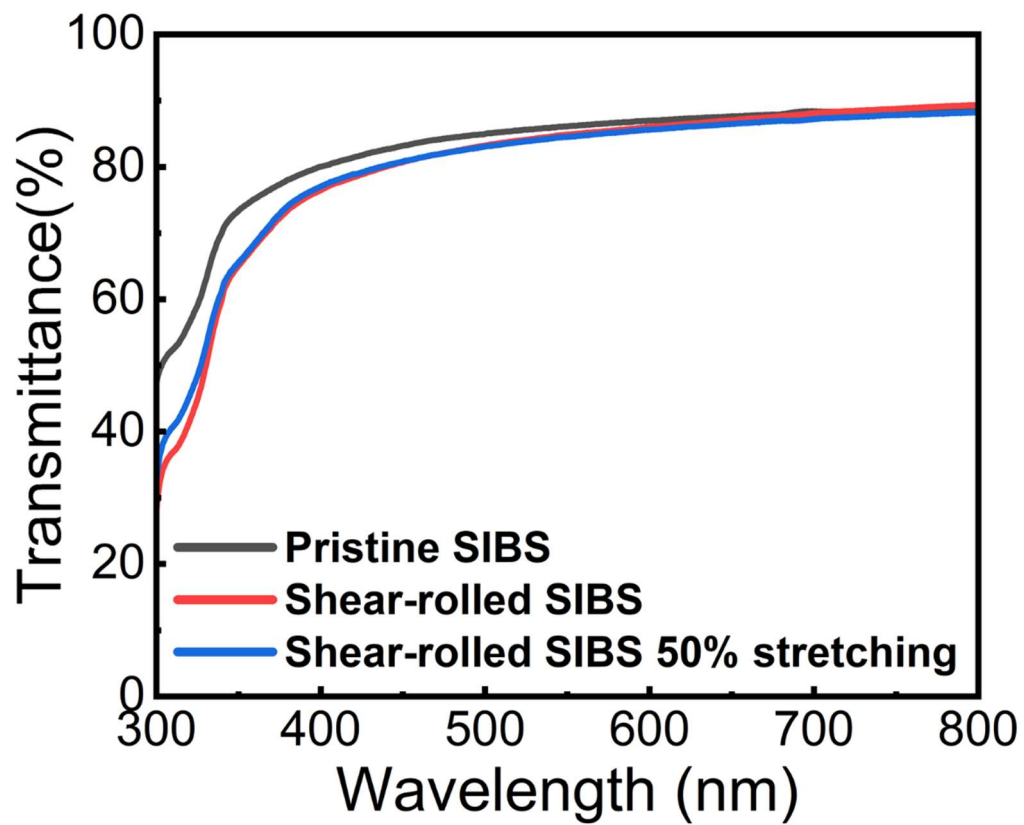


**Figure S4.** Whole strain-stress curve of the 180 °C shear rolled SIBS in alignment and perpendicular directions and the pristine SIBS until fracture

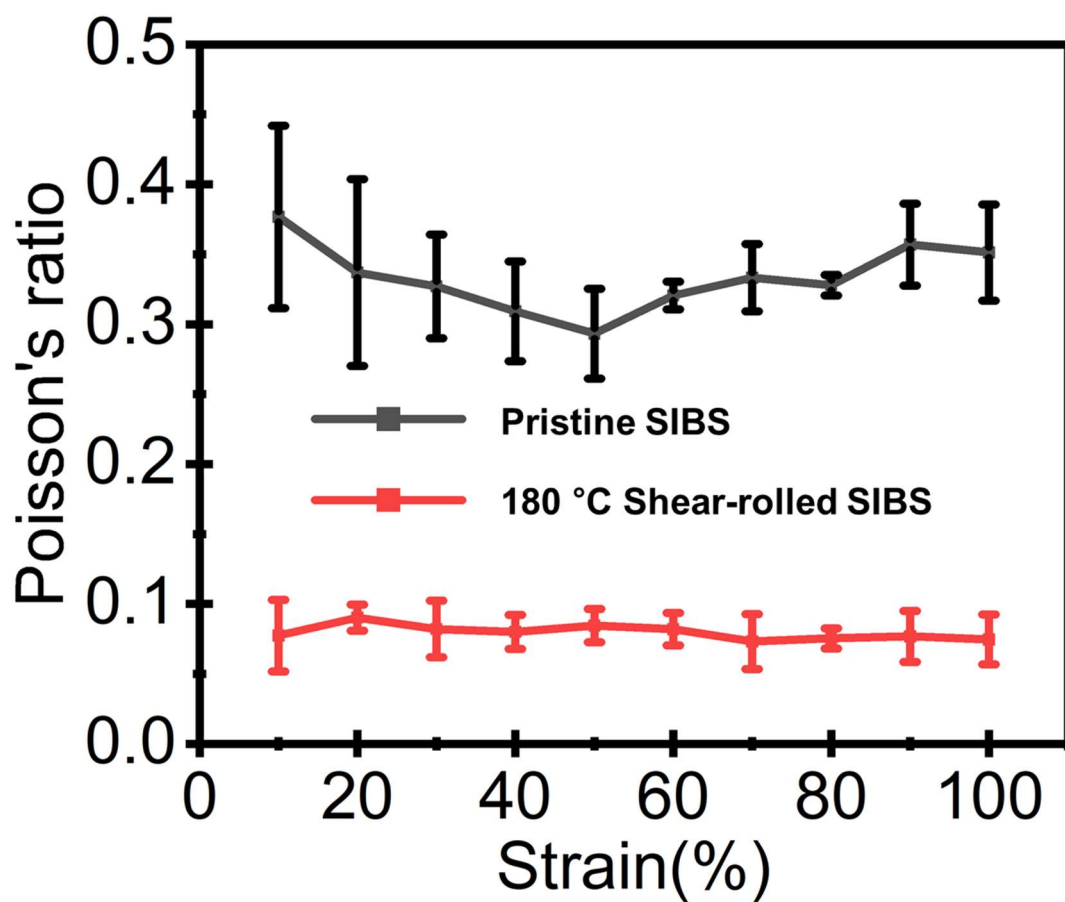
Strain	Pristine SIBS	180 °C Shear-rolled SIBS
0%		
30%		
40%		
50%		
60%		
80%		

**Figure S5.** Photographs of the non-stretched Pristine and the 180 °C shear-rolled SIBS film, and the comparison of vertical deformation between Pristine SIBS film and the 180 °C shear rolled SIBS film at 30%, 40%, 50%, 60% and 80% stretching. The black scale bars in the bottom right of the photographs represent 1cm.

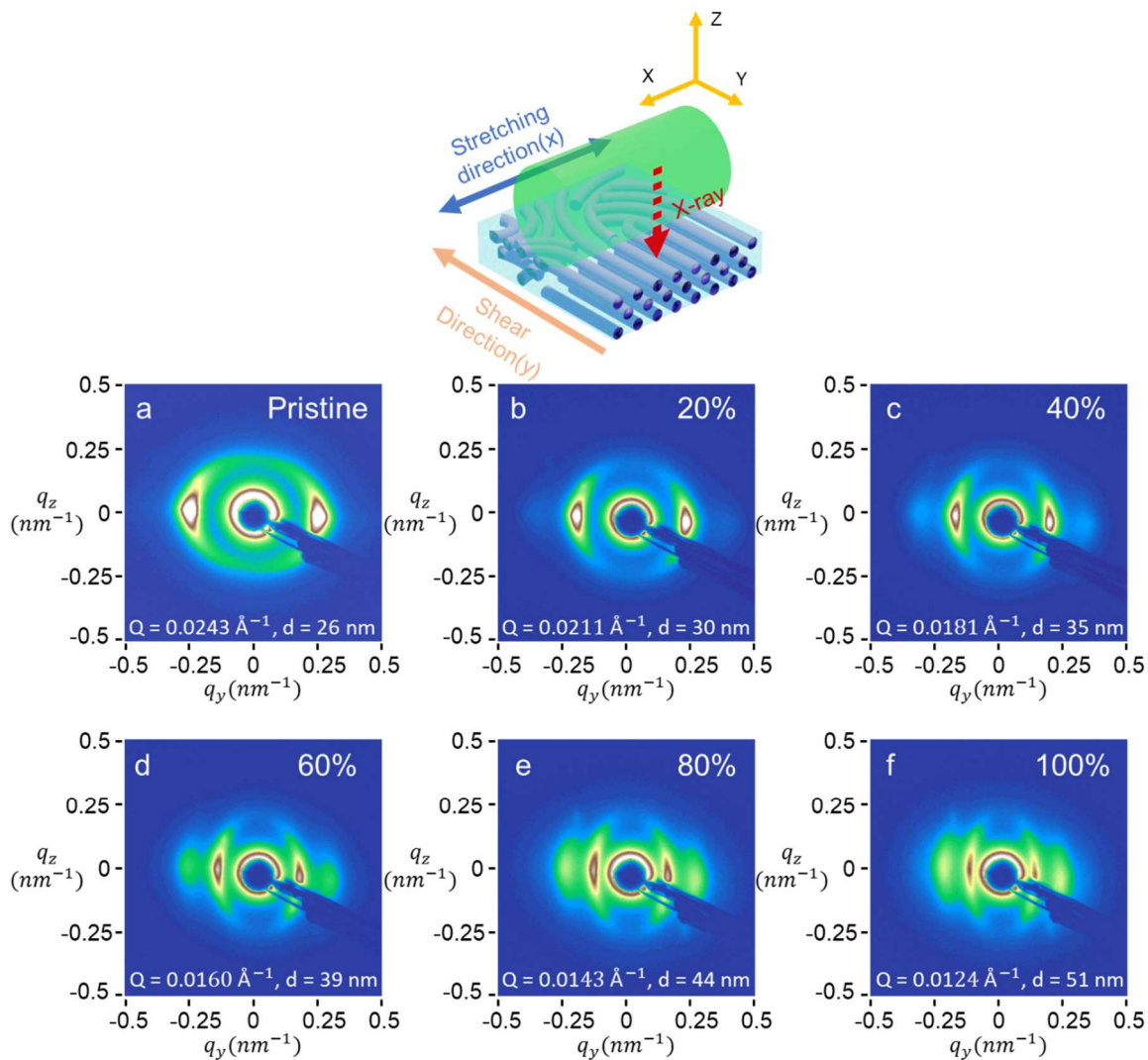




**Figure S6.** The UV-visible spectrum of the Pristine SIBS, shear-rolled SIBS, and 50% stretched shear-rolled SIBS.

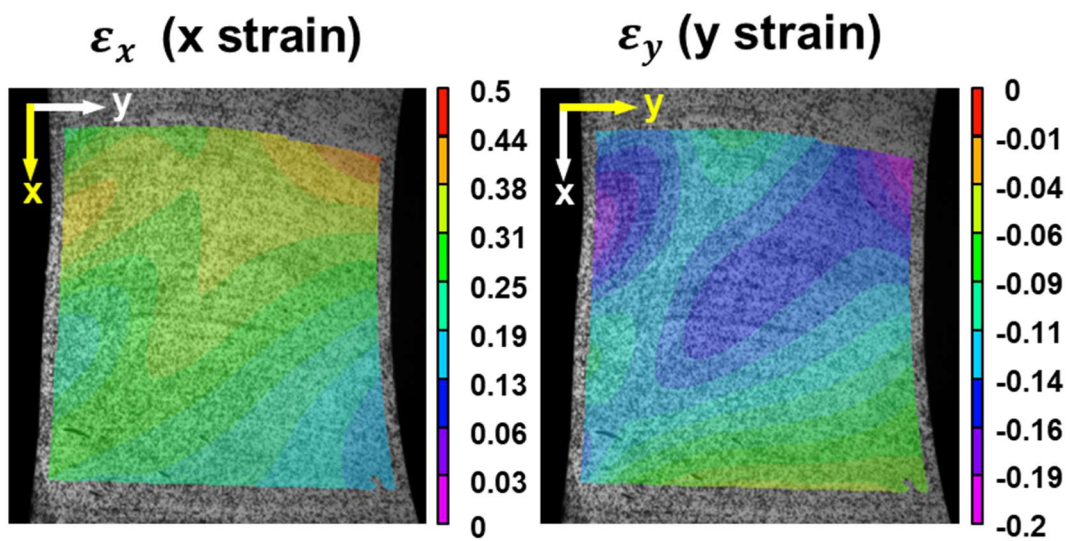


**Figure S7.** Poisson's ratio of the pristine SIBS films and the 180°C shear-rolled SIBS film up to 100% strain

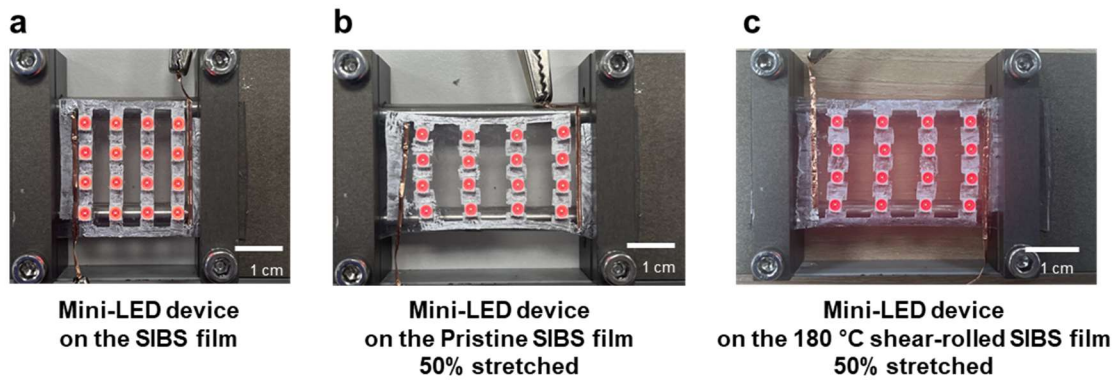


**Figure S8.** Tr-SAXS images of the shear-rolled SIBS film at various strains: (a) before stretching, (b) 20% strain, (c) 40% strain, (d) 60% strain, (e) 80% strain, and (f) 100% strain.

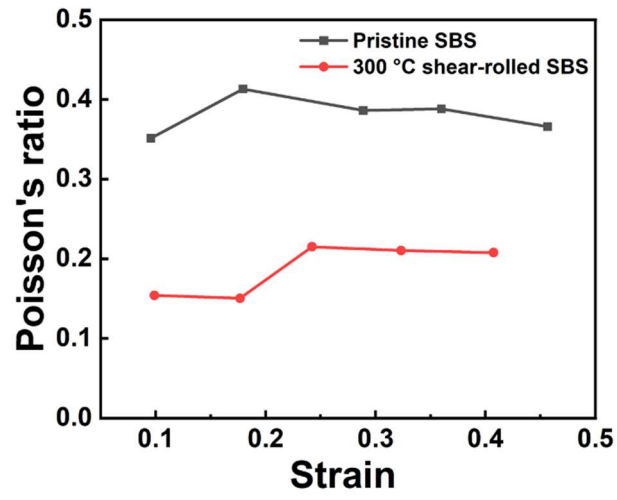
As shown in the schematic at the top, shear stress was applied along the y-axis, the x-ray was directed in the xy-plane, and Tr-SAXS was measured while stretching along the x-axis. In (a), the unstretched film displays a peak at  $0.0243 \text{ \AA}^{-1}$ , corresponding to a d-spacing of 26 nm. Under 20% and 40% strain, the q values decreased to  $0.0211 \text{ \AA}^{-1}$  and  $0.0181 \text{ \AA}^{-1}$ , with d-spacings increasing to 30 nm and 35 nm, respectively in (b-c). At 60%, 80%, and 100% strain, the q values continued to decrease to  $0.0160 \text{ \AA}^{-1}$ ,  $0.0143 \text{ \AA}^{-1}$ , and  $0.0124 \text{ \AA}^{-1}$ , while the d-spacings increased to 39 nm, 44 nm, and 51 nm in (d-f). The d-spacing increased nearly proportionally with strain, and no peaks disappeared or appeared, indicating that the unidirectionally aligned nanocylinder structure remained preserved up to 100% strain.



**Figure S9.** Tr-SAXS images of the shear-rolled SIBS film at various strains: (a) before stretching, (b) 20% strain, (c) 40% strain, (d) 60% strain, (e) 80% strain, and (f) 100% strain.



**Figure S10.** Photographs of the stretchable Mini-LED device connected by an patterned EGaIn circuit form on the SIBS substrate in a bright background. (a) Mini-LED device on the SIBS substrate before stretching (b) Mini-LED device on the pristine SIBS substrate stretched to 50%. (c) Mini-LED device on the 180 °C shear-rolled SIBS substrate stretched to 50%.



**Figure S11.** Poisson's ratio of the Pristine SBS and the 300 °C shear-rolled SBS up to 50% strain.